

Article

Solar Tower Power Plants of Molten Salt External Receivers in Algeria: Analysis of Direct Normal Irradiation on Performance

Abdelkader Rouibah ¹, Djamel Benazzouz ¹, Rahmani Kouider ², Awf Al-Kassir ³ ,
Justo García-Sanz-Calcedo ^{3,*}  and K. Maghzili ⁴

¹ Mechanics Laboratory of Systems and Solids, Faculty of Engineering Sciences (FSI), M'Hamed Bougara University, Boumerdès 35000, Algeria; rouibah_a@yahoo.fr (A.R.); dbenazzouz@yahoo.fr (D.B.)

² Department of Engineering, University of Bab Ezzouar, Algiers 16311, Algeria; kouiderrah1@gmail.com

³ Industrial Engineer School, University of Extremadura, 06006 Badajoz, Spain; aawf@unex.es

⁴ Faculty of technology, Ziane Achour University, Djelfa 17000, Algeria; khaledmeghzili2@gmail.com

* Correspondence: jgsanz@unex.es; Tel.: +34-924-289-600

Received: 3 July 2018; Accepted: 17 July 2018; Published: 25 July 2018



Abstract: The increase of solar energy production has become a solution to meet the demand of electricity and reduce the greenhouse effect worldwide. This paper aims to determine the performance and viability of direct normal irradiation of three solar tower power plants in Algeria, to be installed in the highlands and the Sahara (Béchar, El Oued, and Djelfa regions). The performance of the plants was obtained through a system advisor model simulator. It used real data gathered from appropriate meteorological files. A relationship between the solar multiple (*SM*), power generation, and thermal energy storage (*TES*) hours was observed. The results showed that the optimal heliostat field corresponds to 1.8 *SM* and 2 *TES* hours in Béchar, 1.2 *SM* and 2 *TES* hours for El Oued, and 1.5 *SM* and 4 *TES* hours for Djelfa. This study shows that there is an interesting relationship between the solar multiple, power generation, and storage capacity.

Keywords: solar tower power plants; direct normal irradiation; energy projects; system advisor model

1. Introduction

Algeria highlighted its solar potential where as of the most important heritages in the World, because more than 2 million km² receive an annual insolation of about 2.5 kWh/m² [1,2]. The renewable energy program involves the installation of renewable power of the order of 22 GW by the year 2030 for the national market (i.e., more than 37% of national electricity production with maintaining the export option as a strategic objective) [3].

The world market for solar thermodynamics (CSP) is estimated at 14 GW in 2020 and 72 GW on the horizon of 2035 in very strong growth compared to the capacity installed in 2012 which amounts to 2.8 GW [4]. This strategic choice is motivated by the potential of solar energy from the “Sahara and High Plateau”. This energy constitutes the major axis of the program which is devoted to solar thermal energy [5,6].

The geographic location of Algeria has several advantages to using solar energy. Algeria is situated in the center of North Africa between the 38–35° of latitude north and 8–128° longitude east, and it has an area of 2,381,741 km². The Sahara represents 86% of the area of the country. The climate is transitional between maritime (north) and semi-arid to arid (middle and south).

Solar power systems have a quasi-zero proportional cost: there is no fuel, only expenses (maintenance, guarding, repairs, etc.) which depend very little on the production. However, it is

necessary to take into account its investment costs [7] which are much higher compared to fossil techniques or other renewable energies [8].

In solar tower power plants, since the solar energy is insufficiently dense, it is necessary to concentrate it by means of reflecting mirrors in order to obtain operating temperatures for the production of electricity. The solar radiation can be concentrated on a linear or point receiver. The receiver absorbs the energy reflected by the mirror and transfers it to a thermodynamic heat transfer fluid [9,10].

The performance of the solar system is characterized by its concentration factor. This coefficient makes it possible to evaluate the intensity of the solar concentration [11]. Whenever the concentration factor is high, the temperature reached will be high. Online concentration systems generally have a lower concentration factor less than that of point concentrators [12].

Ho et al. [13] reviewed central receiver designs for concentrating solar power applications with high-temperature power cycles. Boudaoud et al. [14] carried out a technical and economic analysis of electricity costs and the economic feasibility of solar tower power plants in Algeria. Behar et al. [15] evaluated a wide range of clear sky solar radiation models based on theoretical input parameters for the Algerian climate in order to estimate the performance of solar energy projects for which meteorological and radiometric measurement stations are not available. Mihoub et al. [16] proposed a methodology to have an optimal design with a better configuration of the future Algerian solar tower power plants with objectives, the minimization of the electricity costs (LCOE), and the maximization of annual production of electricity.

Quaschnig [17] realized a technical and economic system comparison of photovoltaic and concentrating solar thermal power systems depending on annual global irradiation. He concluded that the electricity generation cost much below 0.10 €/kWh for solar thermal systems and about 0.12 €/kWh for solar photovoltaic can be expected in 10 years in North Africa. In addition, Zhu et al. [18] concluded that introduction of a solar tower field increasing leveled cost of electricity; it contributes to the reduction of CO₂ capture cost compared to the case of standard coal-fired power plants.

Toro et al. [19] studied the thermo-economic design evaluation and optimization of the Central Receiver Concentrated Solar Plants, allowing for improvement of the thermodynamic and economic efficiency of the systems, as well as decreasing the exergy and exergy-economic cost of their products.

Eddine Boukelia et al. [20] made a review of considerations on the assessments for concentrating solar power potential of Algeria. The analysis showed the competitive viability of CSP plants. Algeria has the key prerequisites to make economical CSP power generation, including high-quality insolation and appropriate land, in addition to water availability and extensive transmission and power grid.

Boudaoud et al. performed a technico-economic assessment of a solar tower power pilot plant located in Tipaza, near Algiers. Using the economical, technical, meteorological, and radiometric data, they have carried a simulation of the solar tower power plants (STPP). The results showed that for a net annual energy of about 1 MW, the leveled cost of electricity is about 0.1/kWh, which is relatively high in comparison with the leveled cost of fossil power plant (0.04/kWh) [21].

Larbi et al. [22] showed that solar chimney power plants can produce from 140 to 200 kW of electricity on a site like Adrar (Algeria) during the year, according to an estimate made on the monthly average of sunning. This production is sufficient for the needs of the isolated areas.

Viebahn et al. studied two virtual sites in Algeria and in Spain; they showed a long-term reduction of electricity generating costs to figures between 4 and 6 ct/kWh in 2050. Although the greenhouse gas emissions of current CSP systems showed a good performance (31 g CO₂-equivalents/kWh) compared with fossil-fired systems (130–900 CO₂-eq/kWh), they could further be reduced to 18 g CO₂-eq/kWh in 2050 [23].

Abbas et al. performed a techno-economic assessment of 100 MW of three types of concentrating solar thermal power plants for electricity generation located in one typical site of the Saharan environment of Algeria (Tamanrasset) [24].

The exploitation of Algeria's solar potential complements rural electrification programs. Currently, the use of renewable energies can reach regions far from the national electricity grid.

The parameters and performance of the solar tower power plants of molten salt external receivers to be installed in the North of Algeria are currently not defined. The savings potential is very high and it is planned to install several plants, without the location yet being defined. Most of the studies focus on the south of Algeria, whose solar radiation is higher than the north.

The aim of this paper is to analyze direct normal irradiation on the performance of solar tower power plants of molten salt external receivers in the North of Algeria to optimize the configuration of concentrating solar power (CSP). A comparison study between the three power stations located in the Algerian regions of Béchar, El Oued, and Djelfa, was presented. Each plant is equipped with a molten salt storage mode, the receiver is of external type and the implantation of the field of heliostats that has been defined for an annual production of 20 MW.

This research is useful for prioritizing, sizing, and locating new installations and for determining the technical parameters to be used in the construction projects of solar tower power plants of molten salt external receivers. It will also be useful to define the ideal location based on the solar radiation that maximizes the yield of the CSP plant.

2. Methodology

A numerical simulation under a system advisor model (SAM) based on direct normal irradiance (DNI) with real and satellite data was carried out to optimize the parameters characterizing these performances. The influence of these parameters on each other made it possible to choose an optimal CSP configuration.

In the research, SAM software (Version 2017.9.5, National Renewable Energy Laboratory, Golden, CO, USA, 2017) was used. The SAM is a software to model and simulate the performance of energy parameters and the economics of systems to facilitate the decision-making process in the field of renewable energies [25].

The solar radiation intensity is an important factor in the evaluation of CSP plants. Direct normal irradiance is the amount of direct normal solar radiation received per unit area. There are three techniques to assess the evolution of DNI over time for a given location [26,27].

Optimization of the design of the heliostats field is a trade-off between optical performance and cost, so this process includes both optical and economic analysis. This implantation can be performed by determining the optimum values of the radial spacing ΔR and the azimuth spacing ΔA_Z .

There are various optimization procedures to establish these two geometric position parameters. One of the most effective procedures is the radial offset arrangement [28]. The evaluation of the radial and azimuthally distance can be evaluated by empirical Equations (1) and (2) [29]. These parameters also depend on the angle (α) between the heliostat, the ground, and the tower, as shown in Figure 1 [30,31].

$$\Delta R_{HM} = 63.0093 - 0.587313 \cdot \theta + 0.018423909 \cdot \theta^2 + (2.808733 - 0.1480498 \cdot \theta + 0.001489201 \cdot \theta^2) \cdot \cos \alpha \quad (1)$$

$$\Delta A_Z WM = 2.46812 - 0.0401054 \cdot \theta + 0.000923594 \cdot \theta^2 + (0.17344593 - 0.009112590 \cdot \theta + 0.00012761 \cdot \theta^2) \cdot \cos \alpha \quad (2)$$

where ΔR is the radial distance between heliostats (m), HM is the heliostat height meters, θ is the receiver elevation angle from heliostat, α is the heliostat loft angle in degree, ΔA_Z is the azimuthal distance between heliostats (m), and WM is the heliostat width meters (m).

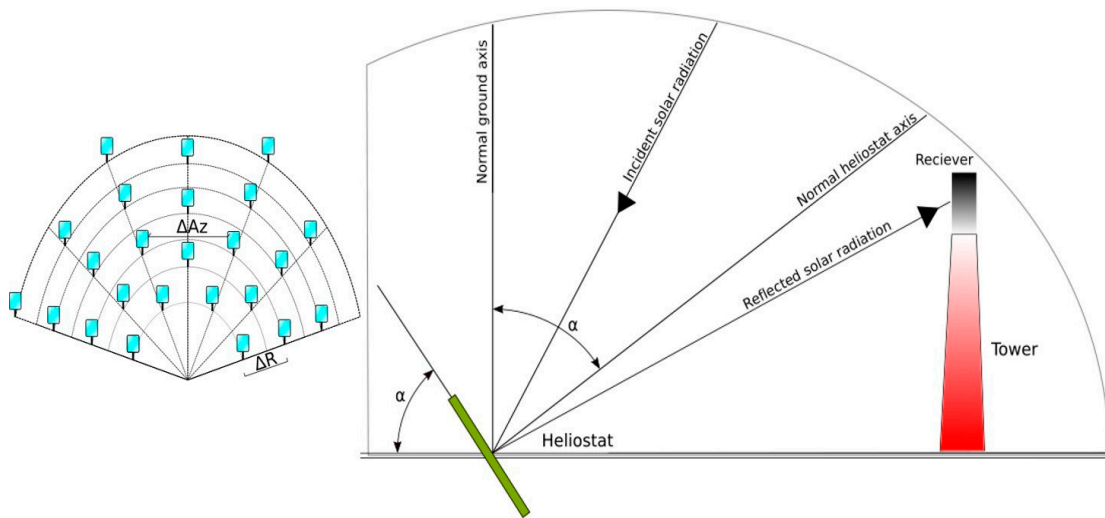


Figure 1. Implementation of the heliostats field. Representation of the optical angle α .

Table 1 shows the location parameters for different regions.

Table 1. Location parameters for different regions.

Parameter	Design Parameters	Djelfa	El Oued	Béchar
Location	DNI (W/m ²)	1050.00	750.00	700.00
	Latitude (°)	34.68	33.50	31.50
	Longitude (°)	3.25	6.78	−2.25
	Elevation (m)	1144.00	69.00	816.00

The size of the heliostat field influences the optical performance and depends on the desired power and temperature of the heat transfer fluid at the output. The total incident thermal energy is given by the following Equation (3):

$$Q_h = I_d \cdot A_h \cdot N_h \tag{3}$$

where I_d is the direct normal irradiation, A_h is the surface of the heliostat, and N_h is the number of the heliostat, and 144 m² was considered the surface of the heliostat field.

The efficiency of the field η_h is defined by the following Equation (4):

$$\eta_h = \frac{Q_{rec}}{Q_{inc}} = \frac{Q_{rec}}{I_d \times A_h \times N_h} \tag{4}$$

where Q_{rec} is the heat flow of the receiver and Q_{inc} is heat flow of the incident.

The efficiency is calculated considering losses due to different effects (cosine, shading, blocking, overflow, reflection, dispersion) and it is given by the following Equation (5) [32]:

$$\eta_h = \eta_{cos} \cdot \eta_{omb} \cdot \eta_{bloc} \cdot \eta_{deb} \cdot \eta_{ref} \cdot \eta_{disp} \tag{5}$$

where η_{cos} is the losses due to cosine effect, η_{omb} is the losses due to shading effect, η_{bloc} is the losses due to blocking effect, η_{deb} is the losses due to overflow; η_{ref} is the losses due to reflection and η_{disp} is the losses due to dispersion.

The model of the receiver of the present study is an external type. It consists of a large number of vertically disposed pipes through which a heat transfer fluid is pumped in the vertical direction. Inside the pipe three types of heat transfer are identified (convection, conduction, and radiation) and

the exchange with the outside by radiation (solar and radiation losses), by convection (losses at the body of the receiver) and by conduction (losses through thermal bridges). Figure 2 shows the different heat exchanges of the receiver with the external environment.

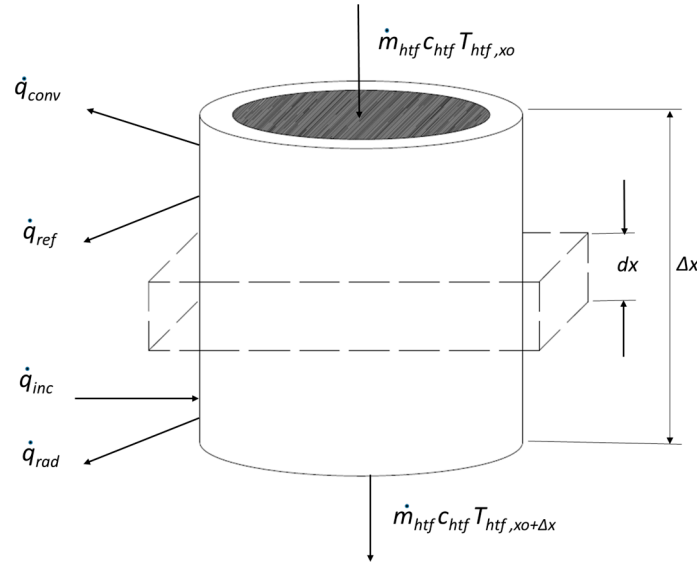


Figure 2. Energy balance of the external receiver.

The heat flux of the receiver can be expressed by Equation (6):

$$Q_{rec} = q_{htf} + q_{conv} + q_{rad} + q_{ref} \tag{6}$$

$$Q_{rec} = S_i \cdot I_d \tag{7}$$

where q_{htf} is the heat flow of molten salt; q_{conv} : loss of convection heat flow; q_{rad} : loss of radiation heat flux; q_{ref} : loss of reflection flux; S_i : total surface.

The incidence of solar radiation I_d on the receiver is evaluated by the flux map radiation model. The distribution of the radiation flux is integrated by combining the effect of the different losses occurring in a heliostats filed layout (cosine effect, shadowing effect, blocking effect, atmospheric attenuation, spillage and flux image profile), based on direct radiation from 950 W/m^2 [26,33]. The energy absorbed by the heat transfer fluid (q_{htf}) is given by the following Equation (8):

$$q_{htf} = m_{htf} \cdot C_{htf} \cdot (T_{htf(x+dx)} - T_{htf(x)}) = US_i \cdot (T_{st} - T_{htf}) \tag{8}$$

$$US_i = \frac{1}{R_{cond} + R_{conv}} \tag{9}$$

$$R_{cond} = \frac{\ln \frac{D_{ot}}{D_{it}}}{2 \cdot \pi \cdot L_t \cdot K_t \cdot N_t} \tag{10}$$

$$R_{conv} = \frac{2}{\pi \cdot h_{htf} \cdot L_t \cdot D_t \cdot N_t} \tag{11}$$

where q_{htf} is the heat flow of molten salt (W), m_{htf} is the molten salt flow rate (kg/s), C_{htf} is the heat capacity of the molten salt fluid (kJ/kg·K), T_{htf} is the inlet temperature of the molten salt at x position (K), US_i is heat transfer conductance coefficient (W/K), T_{st} is receiver temperature at the surface (K), R_{cond} is heat transfer resistance by conduction (K/W), R_{conv} is heat transfer resistance by convection (K/W), D_{ot} is outer diameter of the tube (m), D_{it} is the inner diameter of the tube (m), L_t is

length of the tube (m), K_t is thermal conductivity of the receiver tube (W/m·K), N_t is total number of the receiver tube, and D_t diameter of the tube (m).

The losses by convection are given by Equation (12):

$$q_{conv} = S_i \cdot h_{conv} \cdot (T_{st} - T_{ic-air}) \quad (12)$$

where q_{conv} is the loss of convection heat flux (W), S_i is total surface/Surface total (m²), h_{conv} is the convective heat losses from each receiver tube (W/m²·K), T_{st} is the receiver temperature at the surface (K), and T_{ic-air} is the temperature of the air in the inner cavity (K).

The radiation losses q_{rad} have a negligible value because the absorber has a high absorption of short waves of solar radiation and the same for losses by reflection q_{ref} due to the less emissivity of the long thermal waves.

The performance of a good configuration of the solar tower system is based on several parameters such as power generation injected to the grid, incident solar radiation, and storage capacity. The capacity factor and the multiple solar characterizing the performance of a central solar tower system.

The ratio of the energy generated by the system in partial time E_{gp} and the energy generated in full-time E_{gf} determines the capacity factor [27] and is given by Equation (13):

$$CF = \frac{E_{gp}}{365.24 \cdot E_{gf}} \quad (13)$$

where CF is capacity factor, E_{gp} is the energy generated in part-time (W), and E_{gf} is the energy generated in full-time (W)

The ratio of energy to design point (thermal power produced by the field of heliostats q_{sf} for different DNI values), and the thermal power required by the power block under nominal conditions q_{pb} determines the solar multiple (SM). It is expressed by Equation (14), [34].

$$SM = \frac{q_{sf}}{q_{pb}} \quad (14)$$

where SM is solar multiple factor, q_{sf} is the energy generated by the field of heliostats (W), and q_{pb} is the energy required by the power block (W). For a system without a storage mode, $SM = 1$.

Table 2 shows component characteristics and design parameters of the solar tower system used in the research.

Annual meteorological database that known as the reference year test (TRY) or typical meteorological year (TMY) was used. It consists of measured values, which are statistically selected from the annual individual values measured over a long period. The file formats used are file extensions: TMY2, TMY3, EPW, and CSV. To optimize the performance of the solar tower system of different regions, one needs to optimize the solar fields by the variation of the solar multiple (SM) in function of thermal energy storage (TES) hours, in order to optimize the dimensions of the system and maximize the production of electricity and the capacity factor of the solar tower system.

Table 2. Characteristics of the components of the solar tower system.

Parameter	Design Parameters	Value
Field of heliostats	Surface of the heliostat (m ²)	144.00
Tower and receiver	Diameter of pipes (mm)	60.00
	Thickness of pipes (mm)	1.25
	Type of pipe material (stainless steel)	
Fluid	Heat transfer fluid (HTF) type	60% NaNO ₃ , 40% KNO ₃
Coolant	Input temperature (°C)	565.00
	Output temperature (°C)	290.00
Power block	Design turbine output (MWe)	820.00
	Thermodynamic cycle efficiency (%)	37.00
	Operating pressure of the boiler (bar)	100.00
	Type of cooling capacitor	Air
Energy storage	Type of storage	2 tanks
	Load storage in full hours	0–12 h

3. Results

The results obtained in the research, grouped according to the regions analyzed, are as follows.

3.1. Region of Béchar

In Figure 3a, it can be observed that the electrical production per square meter of heliostats increase proportionally with the SM except the decrease recorded in the interval (1.4–1.5) due to the increase in the surfaces of the heliostats mirrors and the decrease in the length of the tower, which are influenced by the losses due to the effects of the heliostat field as indicated in Figure 3b. Beyond SM = 1.6, the increase in the solar field area has no influence on the evolution of electrical production which converges and increases slightly due to the effects corresponding to the enormous expansion of the solar field and atmospheric attenuation.

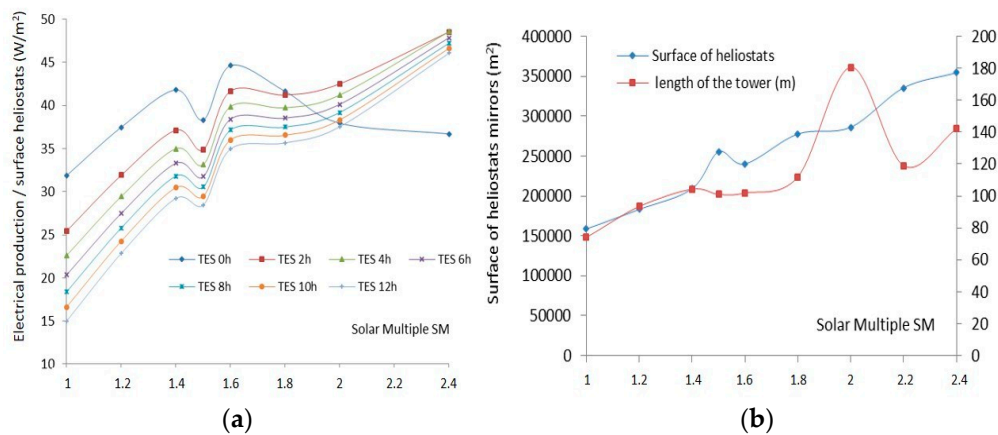


Figure 3. (a) Solar multiple effect (SM) on electrical production/surface heliostats under different values of TES (Béchar). (b) Solar multiple effect on the surface of the heliostats mirrors and length of the tower (Béchar).

For SM values of 2.0, 2.2, and 2.4, the electrical production per m² increases until the peak values: 42.53 W/m², 47.07 W/m², and 48.55 W/m² for TES = 2 h, then it decreases as explained in Figure 4. The configuration of the plant in these values requires a large area, which is not profitable. Therefore,

the electrical production at the start of the system for $SM = 1.8$ is larger, lowers slightly to $TES = 2$ h, and then coincides with the curve corresponding to $SM = 1.6$.

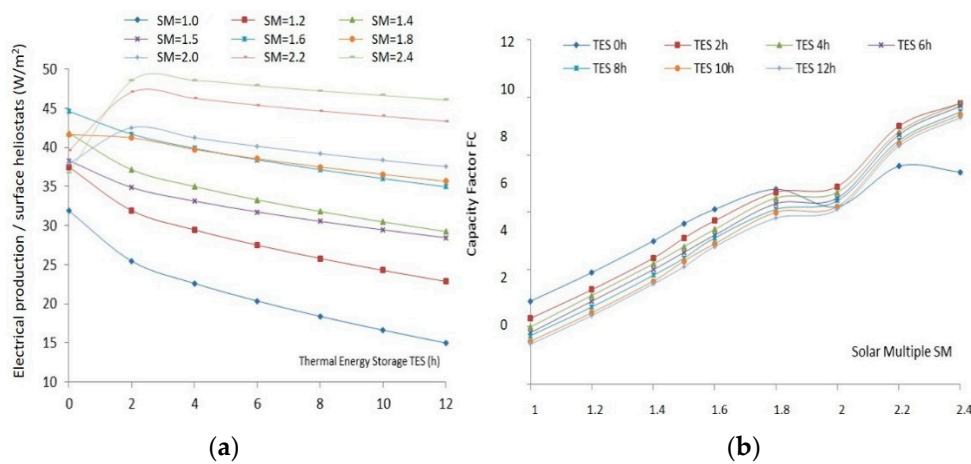


Figure 4. (a) Effect of Thermal Energy Storage (TES) on electrical production/ m^2 (surface heliostats) under different values of solar multiple (Béchar). (b) Solar multiple effect on capacity factor (CF) under different TES values (Béchar).

3.2. Region of El Oued

The capacity factor CF evolves proportionally with the SM . The graphs converge towards close values as shown in Figure 5. Except for the graph corresponding to $TES = 0$ h and $SM = 2.2$, which begins to descend slightly, this decrease is due to the loss of excess of the non-stored energy received by the receiver. From above, it can be concluded that the optimal point of operation of the system corresponds to the following coordinates: $SM = 1.8$, $TES = 2$ h, and the electrical production is 11.44 GWh/year.

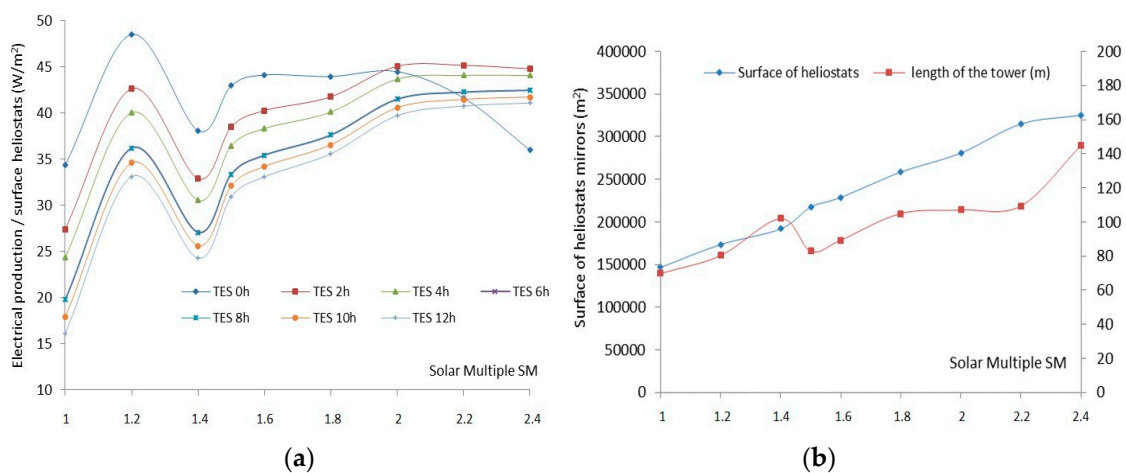


Figure 5. (a) Solar multiple effect (SM) on electrical production per surface heliostats under different values of TES . (b) Solar multiple effect on the surface of heliostats mirrors (m^2) and length of the tower (m).

In Figure 5a, it can be seen that the electrical production per square meter of heliostats increase proportionally with the SM , except that there is a decrease recorded in the interval (1.2–1.4), where the length of the tower has exceeded the surface of the corresponding heliostat mirrors and then decreases to the value of 80 m, to resume the increase in electrical production in the interval (1.4–1.5), as shown

in Figure 5b. Beyond $SM = 1.5$, the curves of electrical production continue parallel to their growth but it keeps constant the value of the electrical output at $SM = 1.2$ and view the optimal surface of the solar field.

For $SM = 2.0, 2.2,$ and 2.4 , the electrical production per m^2 increases until to peak values: $45.07 W/m^2, 45.18 W/m^2,$ and $44.79 W/m^2$ for $TES = 2$ h then it drops as explained in Figure 6a. The configuration of the plant in these values requires a large area of the heliostat field, which is not profitable. Consequently, the electrical production at the start of the system for $SM = 1.2$ is greater, drops slightly up to $TES = 2$ h and then coincides with the curve corresponding to $SM = 1.8$.

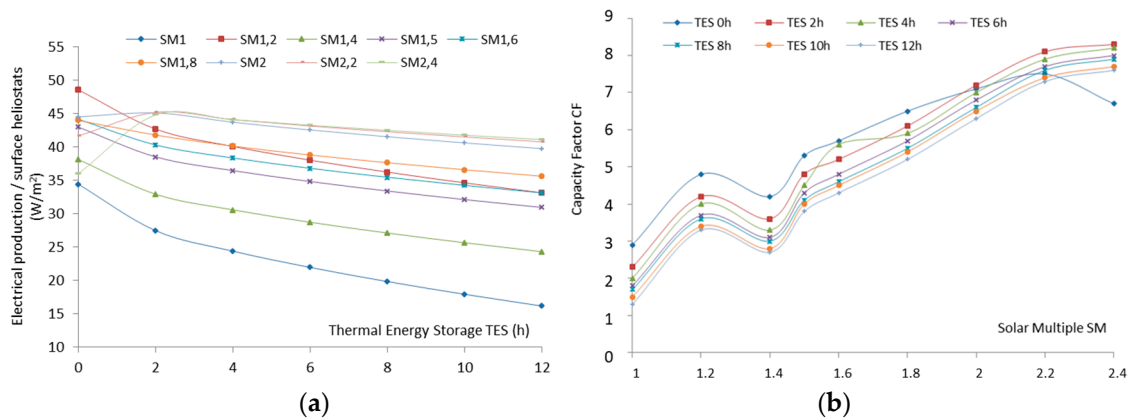


Figure 6. (a) The effect of Thermal Energy Storage (TES) on electrical production/ m^2 (surface heliostats) under different values of solar multiple. (b) The solar multiple effect on capacity factor (CF) under different TES values.

The capacity factor (CF) evolves proportionally with the solar multiple (SM), the curves increase in parallel and tend towards close values as shown in Figure 6b, except for the curve corresponding to $TES = 0$ h and $SM = 2.2$ which begins to descend slightly; this decrease is due to the loss of excess of the non-stored energy received by the receiver.

From above, it can be concluded that the optimal point of operation of the system corresponds to the following coordinates $SM = 1.2, TES = 2$ h and the electrical production is 7.4 GWh per year.

3.3. Region of Djelfa

In Figure 7, the following variations can be distinguished. For $TES = 0$ h to 4 h, the electrical production per square meter of the heliostats increase respectively with the values $SM = 1.2, SM = 1.6,$ and $SM = 2,$ and then it decreases; for $TES = 6$ h to 12 h, the electrical production per square meter of the heliostats increase proportionally with to a converging value; for $SM = 2.0, 2.2,$ and 2.4 , the electricity production per m^2 of heliostat's increases proportionally with the TES . For the other SM , the electrical production increases until $TES = 2$ h, then it decreases. Except for $SM = 1.8$, the electrical production is interesting as TES exceeds 4 h. The configuration of the system becomes unprofitable (a large area, large dimensioning of the tower). On the other hand, the starting power of the plant is much better for $SM = 1.5$ and remains almost stable from $TES = 4$ h.

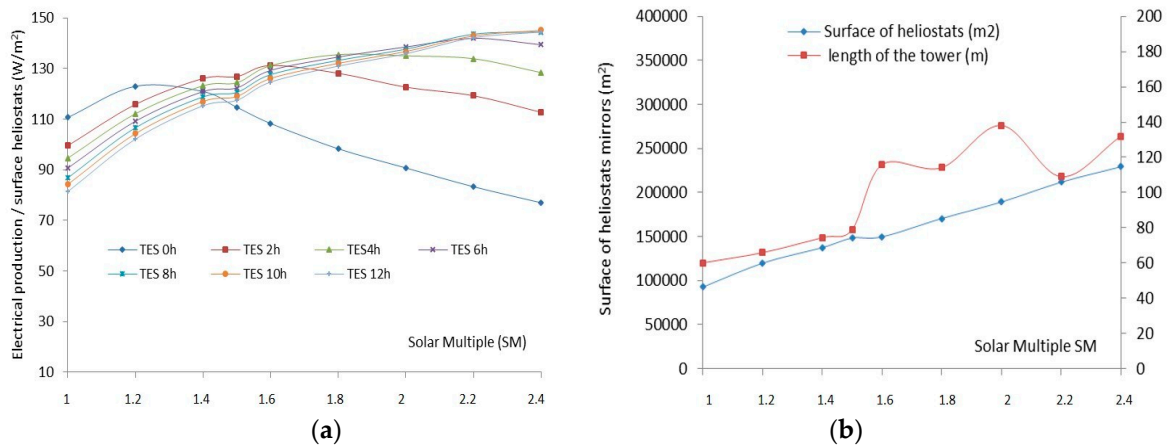


Figure 7. (a) Solar multiple effect (*SM*) on electrical production by surface heliostats under different values of *TES*. (b) Solar multiple effect on the surface of the heliostats mirrors (m^2) and the length of the tower (m).

The capacity factor (*CF*) evolves proportionally with the solar multiple (*SM*), the curves increase proportionally and tend towards close values except for *TES* = 0 h, 2 h and 4 h as shown in Figure 8.

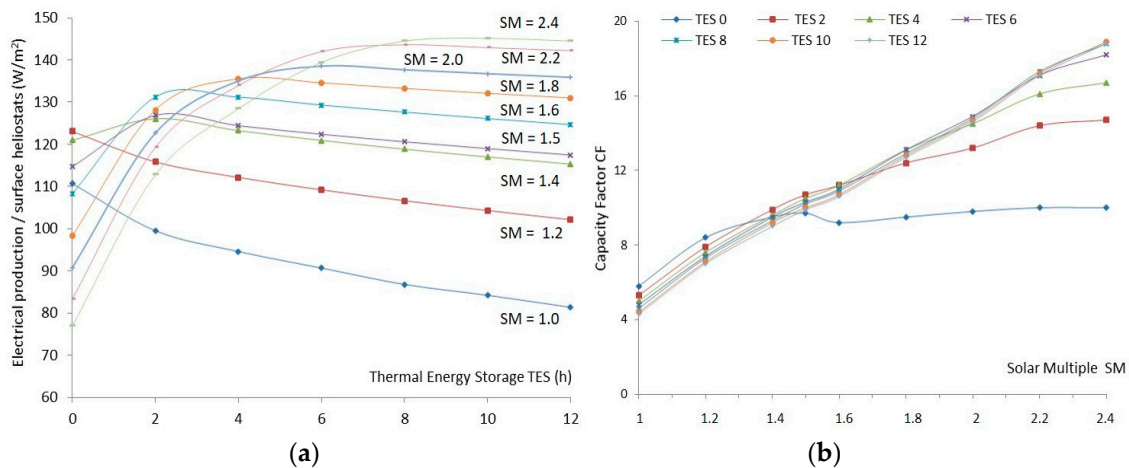


Figure 8. (a) Effect of Thermal Energy Storage (*TES*) on electrical production/ m^2 (surface heliostats) under different values of solar multiple (*Djelfa*). (b) The solar multiple effect on capacity factor (*CF*) under different *TES* values (*Djelfa*).

From above, it can conclude that the optimal point of operation of the system corresponds to the following coordinates $SM = 1.5$, $TES = 4$ h, and the electrical production is 18.45 GWh/year. Table 3 shows the model validation parameters simulated in Djelfa and Batna.

Table 3. Parameters of the model validation.

Type of Parameter	Simulated Case, Scenario 1 [14]	Simulated Case, Scenario 2 [14]	Simulated Case, Study
Annual DNI (kWh/m^2)	1907.30	1907.30	2416.30
Hybridization (%)	0.00	15.00	0.00
Net energy production (GWh/year)	18.15	44.40	18.45
Net energy production difference (%)			1.60 (scenario 1.00 and study)
Annual capacity factor (%)	10.60	26.00	10.50

3.4. Optimization of the Field of Heliostats

From the above, for the optimal points of operation of CSP system of the three regions, it can conclude that the optimal heliostat field corresponds to the solar multiple and storage hours: $SM = 1.8$, $TES = 2$ h for Béchar region; $SM = 1.2$, $TES = 2$ h for El Oued region; and $SM = 1.5$, $TES = 4$ h for Djelfa region. The simulation results are shown in Figure 9.

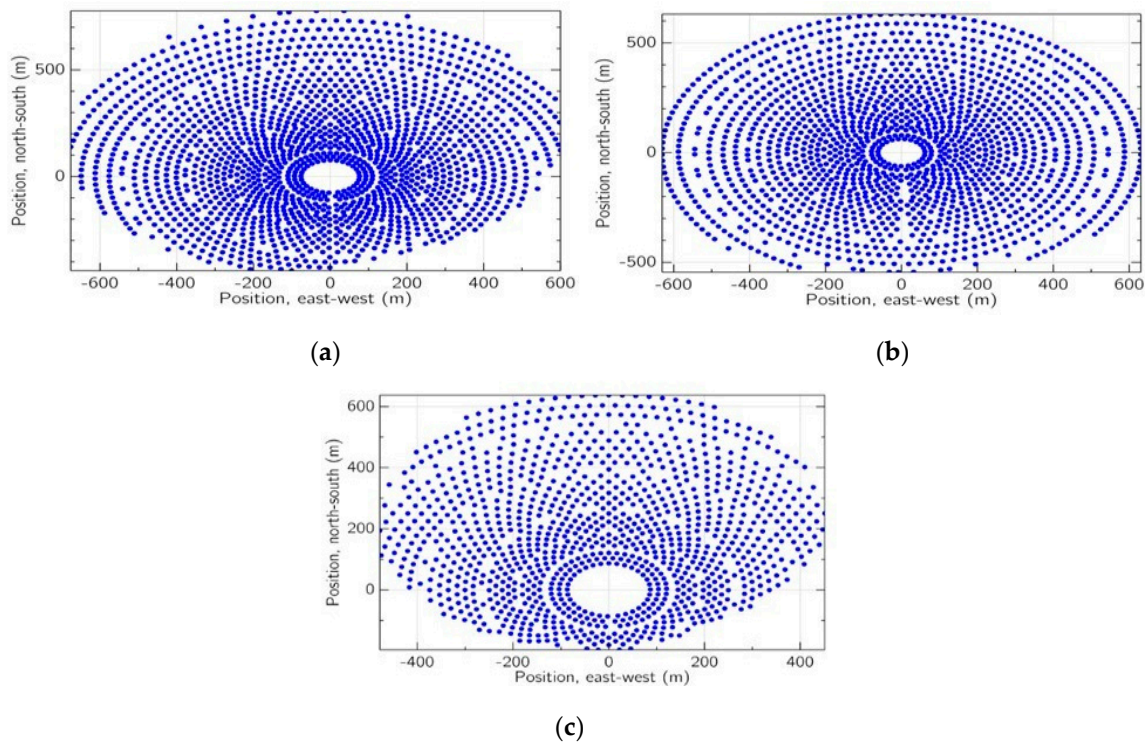


Figure 9. (a) Concentrated Solar Power (CSP) heliostats field configuration of Béchar region. (b) CSP heliostats field configuration of El Oued region. (c) CSP heliostats field configuration of Djelfa region.

Figure 9 shows how the largest STE was produced in the Djelfa region, although the highest SM was found in the CSP heliostat field configuration of Béchar region.

4. Discussion

Algeria is one of the most suitable countries for the cheap production of electricity from solar energy sources, especially from solar thermal concentration technology. Despite the great virtues of solar energy, the development of technologies that allow its use has been gradually slowed down by its disadvantages, including its high investment costs and the impossibility of generating energy at times when there is no solar radiation or it is intermittent due to the passage of clouds.

This study researches the influence of solar normal irradiation on solar power plants and its efficiency. It simulates the electricity production, capacity factors, and surface area required for solar field versus solar multiples considering the effect of TES at different capacities. The study focuses on optimization of CSP heliostat field configuration. Prediction of the field area and solar multiple can directly increase the efficiency of the solar power plant and power production rate. Also, the accumulation of energy through molten salt systems is an adequate solution to promote the use of solar energy.

According to study of the German Aerospace Centre (DLR), Algeria has with 1,787,000 km² of Sahara desert, the largest long-term land potential for concentrating solar thermal power plants. The insolation time over the quasi-totality of the national territory exceeds 2000 h annually, and may

reach 3900 h (High Plains and Sahara) [35]. The daily obtained energy on a horizontal surface of 1 m² is of 5 kWh over the major part of the national territory, or about 1700 kWh/m² per year for the north and 2263 kWh/m² per year for the south of the country [36].

The solar thermal power plant is one of the promising renewable energy options to substitute the increasing demand of conventional energy [37]. The design of the solar towers allows the collector to reach a higher temperature than the cylindrical-parabolic ones. This higher temperature allows for more efficient conversion to electricity, as well as cheaper storage of thermal energy for later use.

The position of heating head is an important factor for power collection. If the sunlight can be concentrated to completely cover the heating head with small heat loss, it can obtain the maximum temperature of the heating head of the Stirling engine. Therefore, the temperature of heating head can be higher than 1000 °C on a sunny day [38].

The choice of the solar field is a difficult exercise, for example, a choice of solar multiples between 1.4 and 1.6 is suitable for high-optical performance with a lower surface of the field, and the starting arrangement must be very close to the optimum configuration, based on the experience obtained from the plants already in operation [39]. The thermal energy storage capacity is insufficient for the whole night, it covers between two and four hours hence the obligation to use an auxiliary energy source.

The starting layout must be very close to the optimum configuration (length of the tower, surface of the mirrors, dimension of the receiver), it is important therefore looking to design a cheaper and better performing heliostat concentrator.

In terms of direct solar irradiance, a measure of the gross energy received per unit area, Algeria is one of the most suitable countries for the cheap production of electricity from solar sources, especially from solar thermal concentration technology [40]. On the other hand, a reduction of taxes decreases leveled cost of electricity generated by CSP solar technologies [41].

However, it should be borne in mind that the type of geometry used in the construction of the reflective surface of a heliostat has a significant influence on the shape and size of the image generated in the plane of the receiver, and therefore on the energy density and the amount of energy intercepted by this element [42].

Concentrating solar power is clean and reliable, can be produced during high demand, and has the potential to meet a country's growing needs in the future. In addition, thermal storage systems prevent fluctuations in supply, allow production to continue in the absence of solar radiation, when direct generation is not possible, and allow production peaks to be transferred in accordance with demand requirements [43].

The research carried out in this work will be useful to optimize the performance of solar tower power plants of molten salt external receivers and to plan its design properly [44]. The results can hopefully help the Algerian government to decide on policies related to performance of solar tower power plants of molten salt external technologies. It has been proven that although energy production is lower in the northern regions of Algeria, it is profitable and allows for the efficient supply of electricity to regions that do not currently have electricity grids.

As prospects for future research, it will use the performance of the solar advisor model for integrating financial modeling into project models. It is also advisable to evaluate the incorporation of a wind barrier in the perimeter of the CSP in order to protect the components from high wind levels and the dust it carries. The barrier protects the heliostats from bursts and prevents the continuous movement of sand that may enter the solar field and deposit on the components.

5. Conclusions

A comparison study between three power stations located in the Algerian regions of Béchar, El Oued, and Djelfa was developed. Each plant is equipped with a molten salt storage mode, the receiver is of external type, and the implantation of the field of heliostats which have been defined for an annual production of 20 MW. It became evident that the regions in Northern Algeria are suitable for the production of concentrated solar energy,

It was found that the system advisor model software is a suitable tool to calculate normal direct irradiation on the performance of solar tower power plants of molten salt external receivers. The use of this software was very interesting in the study. It was observed that direct normal irradiation is a fundamental factor in order to choose an adequate region. High values correspond to a high performance of the solar power plant, resulting in high production and storage capacity.

The results showed that the optimal heliostat field corresponds to 1.8 *SM* and 2 *TES* hours in Béchar, 1.2 *SM* and 2 *TES* hours for El Oued, and 1.5 *SM* and 4 *TES* hours for Djelfa. Therefore, thermodynamic plants should be studied through their direct normal irradiation instead of global horizontal irradiation and diffuse horizontal irradiation.

Finally, this study shows that there is a strong and direct relationship between *SM*, power generation, and storage capacity hours. The higher value of *SM* corresponds to higher values of production and storage capacity. Since the storage hours do not cover the whole night, it is essential either to increase the number of heliostats, and therefore factor *SM*, or provide an auxiliary source of energy to guarantee permanent activity for 24 h.

As lessons learned, it became evident that satellite meteorological data give better results compared to actual data, as electricity production can be twice as high as actual data because the latter take into account atmospheric conditions (clouds, wind, pollution, etc.).

It was found that the system advisor model software is a suitable tool to calculate normal direct irradiation on the performance of solar tower power plants of molten salt external receivers. The use of this software was very interesting in the study. It is observed that direct normal irradiation is a fundamental factor in order to choose an adequate region. High values correspond to a high performance of the solar power plant, resulting in high production and storage capacity.

Author Contributions: Conceptualization, A.R.; Data curation, K.M.; Formal analysis, J.G.-S.-C.; Funding acquisition, D.B.; Investigation, A.R.; Methodology, D.B. and R.K.; Project administration, K.M.; Resources, R.K.; Supervision, A.A.-K. and J.G.-S.-C.; Validation, K.M.; Visualization, A.A.-K.; Writing-original draft, A.R.; Writing-review & editing, D.B.

Funding: This research received no external funding.

Acknowledgments: The authors of the present study would like to express their thankfulness to the financial support of Junta de Extremadura to a part of this study related to Research Projects GR-18029 and 18086, linked to the VI Regional Plan for Research, Technical Development, and Innovation from the Junta de Extremadura 2017-2020.

Conflicts of Interest: The authors declare no conflict of interest.

Nomenclature

<i>STPP</i>	Solar tower power plants
<i>DNI</i>	Direct normal irradiation
<i>DHI</i>	Diffuse horizontal irradiation
<i>GHI</i>	Global horizontal irradiation
<i>SAM</i>	System advisor module
<i>SM</i>	Solar multiple
<i>TES</i>	Thermal energy storage (h)
<i>CSP</i>	Concentrated solar power
ΔR	Radial distance between heliostats (m)
ΔA_Z	Azimuthal distance between heliostats (m)
θ	Receiver elevation angle from heliostat ($^\circ$)
α	Heliostat loft angle in degree ($^\circ$)
A_h	Surface heliostat (m^2)
I_d	Irradiation direct normal (W/m^2)
N_h	Number of heliostats.
η_h	Efficiency of the solar field
η_{cos}	Loss due to cosine effect
η_{omb}	Loss due to shading effect

N_t	Total number of the receiver tube
η_{bloc}	Loss due to blocking effect
η_{deb}	Loss due to overflow
η_{ref}	Loss due to reflection
η_{disp}	Losses due to dispersal
CF	Capacity factor
E_{gp}	Energy generated in part-time (W)
E_{gf}	Energy generated in full-time (W)
TM _Y	Typical Meteorological Year
Q_{rec}	Heat flow of the receiver (W)
Q_{inc}	Incident heat flow (W)
q_{ra}	Loss of radiant heat flux (W)
q_{conv}	Loss of convection heat flux (W)
q_{ref}	Loss of reflection flow (W)
q_{sf}	Energy generated by the field of heliostats (W)
q_{pb}	Energy required by the power block (W)
Q_h	Heat flow of molten salt (W)
S_i	Total surface/Surface total (m ²)
US_i	Heat transfer conductance coefficient (W/K)
m_{htf}	Molten salt flow rate (kg/s)
C_{htf}	Heat capacity of the molten salt fluid (kJ/kg·K)
T_{st}	Receiver temperature at the surface (K)
T_{htf}	Inlet temperature of the molten salt at x position (K)
T_{ic-air}	Temperature of the air in the inner cavity (K)
R_{conv}	Heat transfer resistance by convection (K/W)
R_{cond}	Heat transfer resistance by conduction (K/W)
D_{it}	Inner diameter of the tube (m)
D_{ot}	Outer diameter of the tube (m)
h_{htf}	Convection heat transfer of the molten salt (W/m ² ·K)
h_{conv}	Convective heat losses from receiver tube (W/m ² ·K)
K_t	Thermal conductivity of the receiver tube (W/m·K)
L_t	Length of the tube (m)
TRY	Test Reference Year
EPW	Energy Plus Weather
CSV	Comma Separated Value
WM	Heliostat width meters
HM	Heliostat height meters
HTF	Heat transfer fluid

References

1. Boudghene, S.; Khiat, Z.; Flazi, S.; Kitamura, Y. A review on the renewable energy development in Algeria: Current perspective, energy scenario and sustainability issues. *Renew. Sustain. Energy Rev.* **2012**, *16*, 4445–4460. [CrossRef]
2. Stambouli, A.B. Promotion of renewable energies in Algeria: Strategies and perspectives. *Renew. Sustain. Energy Rev.* **2011**, *15*, 1169–1181. [CrossRef]
3. Energies Nouvelles, Renouvelables et Maitrise de l'Énergie. Available online: <http://www.energy.gov.dz/francais/index.php?page=energies-nouvelles-renouvelables-et-maitrise-de-l-energie> (accessed on 22 May 2018).
4. Medium Term RE Market Report, Agence Internationale de l'Énergie. 2013. Available online: <https://www.iea.org/publications/freepublications/publication/2013MTRMR.pdf> (accessed on 22 May 2018).
5. Ghezloun, A.; Chergui, S.; Oucher, N. Algerian energy strategy in the context of sustainable development (Legal framework). *Energy Procedia* **2011**, *6*, 319–324. [CrossRef]

6. Portail Algérien des Energies Renouvelables. Available online: <https://portail.cder.dz/spip.php?article4446> (accessed on 22 May 2018).
7. Imadojemu, H.E. Concentrating parabolic collectors: A patent survey. *Energy Convers. Manag.* **1995**, *36*, 225–237. [[CrossRef](#)]
8. Hocine Moussa, B. Thermal Solar Power Plants in Algeria and Desertec Mega project. In Proceedings of the Le 1erés Journées d’Etudes de Mécaniques, Batna, Algeria, 29–30 November 2011.
9. Rosen, M.A.; Dincer, I. Exergy–cost–energy–mass analysis of thermal systems and processes. *Energy Convers. Manag.* **2003**, *4*, 1633–1651. [[CrossRef](#)]
10. Adinberg, R. Simulation analysis of thermal storage for concentrating solar power. *Appl. Therm. Eng.* **2011**, *31*, 3588–3594. [[CrossRef](#)]
11. Wellmann, J.; Morosuk, T. Renewable Energy Supply and Demand for the City of El Gouna, Egypt. *Sustainability* **2016**, *8*, 314. [[CrossRef](#)]
12. Annuaire de la Filière Française du Solaire Thermodynamique. 2011. Available online: http://www.enr.fr/userfiles/files/Annuaire/2011/171733_annuairethermo2011.pdf (accessed on 22 May 2018).
13. Ho, C.K.; Iverson, B.D. Review of high-temperature central receiver designs for concentrating solar power. *Renew. Sustain. Energy Rev.* **2014**, *29*, 835–846. [[CrossRef](#)]
14. Boudaoud, S.; Khellaf, A.; Mohammedi, K.; Behar, O. Thermal performance prediction and sensitivity analysis for future deployment of molten salt cavity receiver solar power plants in Algeria. *Energy Convers. Manag.* **2015**, *89*, 655–664. [[CrossRef](#)]
15. Behar, O.; Khellaf, A.; Mohammedi, K. A review of studies on central receiver solar thermal power plants. *Renew. Sustain. Energy Rev.* **2013**, *23*, 12–39. [[CrossRef](#)]
16. Mihoub, S.; Chermiti, A.; Beltagy, H. Methodology of determining the optimum performances of future concentrating solar thermal power plants in Algeria. *Energy* **2017**, *122*, 801–810. [[CrossRef](#)]
17. Quaschnig, V. Technical and economical system comparison of photovoltaic and concentrating solar thermal power systems depending on annual global irradiation. *Sol. Energy* **2004**, *77*, 171–178. [[CrossRef](#)]
18. Zhu, Y.; Zhai, R.; Yang, Y.; Reyes-Belmonte, M.A. Techno-Economic Analysis of Solar Tower Aided Coal-Fired Power Generation System. *Energies* **2017**, *10*, 1392. [[CrossRef](#)]
19. Toro, C.; Rocco, M.V.; Colombo, E. Exergy and Thermo-economic Analyses of Central Receiver Concentrated Solar Plants Using Air as Heat Transfer Fluid. *Energies* **2016**, *9*, 885. [[CrossRef](#)]
20. Boukelia, T.E.; Mecibah, M.S. Parabolic trough solar thermal power plant: Potential, and projects development in Algeria. *Renew. Sustain. Energy Rev.* **2013**, *21*, 288–297. [[CrossRef](#)]
21. Boudaoud, S.; Khellaf, A.; Mohammedi, K. Solar tower plant implementation in northern Algeria: Technico economic assessment. In Proceedings of the 2013 5th International Conference on Modeling, Simulation and Applied Optimization (ICMSAO), Hammamet, Tunisia, 28–30 April 2013; pp. 1–6.
22. Larbi, S.; Bouhdjar, A.; Chergui, T. Performance analysis of a solar chimney power plant in the southwestern region of Algeria. *Renew. Sustain. Energy Rev.* **2010**, *14*, 470–477. [[CrossRef](#)]
23. Viebahn, P.; Lechon, Y.; Trieb, F. The potential role of concentrated solar power (CSP) in Africa and Europe. A dynamic assessment of technology development, cost development and life cycle inventories until 2050. *Energy Policy* **2011**, *39*, 4420–4430. [[CrossRef](#)]
24. Abbas, M.; Merzouk, N.K. Techno economic study of solar thermal power plants for centralized electricity generation in Algeria. In Proceedings of the 2012 2nd International Symposium on Environment Friendly Energies and Applications, Newcastle upon Tyne, UK, 25–27 June 2012.
25. Freeman, J.M.; DiOrio, N.A.; Blair, N.J.; Neises, T.W.; Wagner, M.J.; Gilman, P.; Janzou, S. *System Advisor Model (SAM) General Description (Version 2017.9.5)*; Technical Report for National Renewable Energy Laboratory: Golden, CO, USA, May 2018.
26. Ouagued, M.; Khellaf, A.; Loukarfi, L. Estimation of the temperature, heat gain and heat loss by solar parabolic trough collector under Algerian climate using different thermal oils. *Energy Convers. Manag.* **2013**, *75*, 191–201. [[CrossRef](#)]
27. Gilman, P.; Blair, N.; Mehos, M.; Christensen, C.; Janzou, S.; Cameron, C. *Solar Advisor Model. User Guide for version 2.0*; Technical report NREL/TP-670-43704; August 2008. Available online: <https://www.nrel.gov/docs/fy08osti/43704.pdf> (accessed on 22 may 2018).

28. Kistler, B.L. *A User's Manual for DELSOL3. A Computer Code for Calculating the Optical Performance and Optimal System Design for Solar Thermal Central Receiver Plants*. SAND86-8018. Unlimited release UC-62a. 1986. Available online: <http://ciTESeerx.ist.psu.edu/viewdoc/download?doi=10.1.1.467.8372&rep=rep1&type=pdf> (accessed on 22 May 2018).
29. Ho, C.K. *Overview of Concentrating Solar Power Research at Sandia (Feb 2017)*; Sandia National Lab.: Albuquerque, NM, USA, 2017.
30. Huang, W. Development of an analytical method and its quick algorithm to calculate the solar energy collected by a heliostat field in a year. *Energy Convers. Manag.* **2014**, *83*, 110–118. [[CrossRef](#)]
31. Wagner, M.J. Simulation and Predictive Performance Modeling of Utility Scale Central Receiver System Power Plants. Ph.D. Thesis, University of Wisconsin-Madison, Madison, WI, USA, January 2008.
32. Romero-Álvarez, M.; Zarza, E. Concentrating solar thermal power. In *Handbook of Energy Efficiency and Renewable Energy*; CRC Press: Boca Raton, FL, USA, 2007.
33. Modeling and Calculation of Heat Transfer Relationship for Concentrated Solar Power Receivers. Available online: <https://search.library.wisc.edu/catalog/9910121576302121> (accessed on 30 May 2018).
34. ReGrid: Concentrated Solar Power. (RENAC) Renewables Academy. Schonhauser Alee 10–11. 10119. Berlin, Germany. Available online: <https://www.renac.de/en/projects/> (accessed on 22 May 2018).
35. German Aerospace Centre (DLR). Available online: <https://www.dlr.de/dlr/en/desktopdefault.aspx/tabid-10002/> (accessed on 30 May 2018).
36. Centre de Developpement des Energies Renouvelables (CEDER). Algeria (2013). Available online: <http://www.cder.dz/> (accessed on 2 June 2018).
37. Siva Reddy, V.; Kaushik, S.C.; Ranjan, K.R.; Tyagi, S.K. State of the art of solar thermal power plants. A review. *Renew. Sustain. Energy Rev.* **2013**, *27*, 258–273. [[CrossRef](#)]
38. Cheng, T.C.; Yang, C.K.; Lin, I. Biaxial-Type Concentrated Solar Tracking System with a Fresnel Lens for Solar-Thermal Applications. *Appl. Sci.* **2016**, *6*, 115. [[CrossRef](#)]
39. Ohya, Y.; Wataka, M.; Watanabe, K.; Uchida, T. Laboratory Experiment and Numerical Analysis of a New Type of Solar Tower Efficiently Generating a Thermal Updraft. *Energies* **2016**, *9*, 1077. [[CrossRef](#)]
40. Gregorio-Muñiz, J.M. El Mercado de las Energías Renovables en Argelia. Oficina Económica y Comercial de la Embajada de España en Argel. 2004. Available online: <https://www.icex.es/icex/> (accessed on 2 June 2018).
41. Owen, A.D. Renewable energy: Externality costs as market barriers. *Energy Policy* **2006**, *34*, 632–642. [[CrossRef](#)]
42. Pitz-Paal, R.; Botero, N.B.; Steinfeld, A. Heliostat field layout optimization for high-temperature solar thermochemical processing. *Sol. Energy* **2011**, *85*, 334–343. [[CrossRef](#)]
43. Zhang, H.L.; Baeyens, J.; Degreè, J.; Cacères, G. Concentrated solar power plants: Review and design methodology. *Renew. Sustain. Energy Rev.* **2013**, *22*, 466–481. [[CrossRef](#)]
44. Candelario-Garrido, A.; García-Sanz-Calcedo, J.; Reyes, A.M. A quantitative analysis on the feasibility of 4D planning graphic systems versus conventional systems in building projects. *Sustain. Cities Soc.* **2017**, *35*, 378–384. [[CrossRef](#)]



© 2018 by the authors. Licensee MDPI, Basel, Switzerland. This article is an open access article distributed under the terms and conditions of the Creative Commons Attribution (CC BY) license (<http://creativecommons.org/licenses/by/4.0/>).